



# Computational Design of a Multi-Epitope Vaccine Against Nipah Virus: Bridging Immunoinformatics and Immune Protection

Seerat Fatima<sup>†</sup>, Fatima Jawed<sup>†</sup>, and Shumaila Zulfiqar<sup>\*</sup>

Department of Biotechnology, Kinnaird College for Women, Lahore, Pakistan

**Abstract:** Nipah virus (NiV) is a highly lethal zoonotic paramyxovirus with no licensed vaccines or targeted antiviral therapies, posing a serious global health threat. Recurrent outbreaks in South and Southeast Asia highlight the critical need for efficacious and broadly protective vaccine strategies. In this research, an immunoinformatics-based approach was utilized to construct a multi-epitope vaccine (MEV) targeting the highly conserved NiV fusion protein (NCBI ID: AAY43915.1). The protein exhibited high antigenicity, non-allergenic potential, and favorable physicochemical properties. Cytotoxic T-lymphocyte (CTL), Helper T-lymphocyte (HTL), and B-cell epitopes were predicted and rigorously screened for immunogenicity, non-toxicity, and sequence conservancy, resulting in the selection of epitopes with over 90% identity across Bangladeshi and Malaysian NiV strains. Population coverage analysis confirmed the broad applicability of Human Leukocyte Antigen (HLA), particularly in endemic regions. The finalized MEV construct, incorporating appropriate linkers and a 50S ribosomal protein adjuvant, showed structural stability following modelling, refinement, and validation. Molecular docking revealed strong binding affinity with TLR3 and TLR4. Computational immune simulations predicted robust adaptive immune responses, and codon optimization, along with in silico cloning, confirmed favorable expression in *E. coli*. Although these findings are supported by computational analyses and should be validated experimentally, the proposed MEV demonstrates strong cross-protective and immunogenic potential, offering an encouraging platform for the design of a pan-strain NiV vaccine.

**Keywords:** Nipah Virus, Multi-epitope Vaccine (MEV), Fusion Protein, Molecular Docking, Immunogenicity, Vaccine.

## 1. INTRODUCTION

The Indian subcontinent is a hotspot for zoonotic infections due to dense human-animal interactions, inadequate disease monitoring, and limited public health infrastructure [1]. Among these threats, Nipah virus (NiV) is known to be a highly fatal zoonotic paramyxovirus capable of both animal-to-human, and human-to-human transmission, with mortality rates reaching up to 100% in some outbreaks [2, 3]. Despite multiple outbreaks in Bangladesh, India, and Malaysia, there isn't a licensed human vaccination against NiV at the moment, posing a persistent threat to regional and global health [4, 5].

Nipah virus (NiV) is a membrane-bound negative-sense RNA virus of the genus Henipavirus within the Paramyxoviridae family. Its genome encodes the six structural proteins, of which the fusion protein (F) is essential for viral uptake by

regulating membrane coalescence between the virus and host cells. Given its essential function and relatively conserved nature, the F protein is an attractive target for vaccine development aimed at providing broad-spectrum protection across NiV strains.

Traditional vaccine approaches for NiV, including live-attenuated, viral vector-based, and protein subunit vaccines, are still in clinical or preclinical phases [6]. These strategies face challenges such as biosafety level 4 (BSL-4) restrictions, high production costs, and prolonged development timelines [7, 8]. In contrast, a multi-epitope vaccine (MEV) design using immunoinformatics offers a safer, faster, and more cost-effective alternative for targeting highly pathogenic viruses like NiV [9, 10]. Several in silico studies have previously proposed multi-epitope vaccine (MEV) constructs against NiV,

Received: June 2025; Revised: November 2025; Accepted: December 2025

\* Corresponding Author: Shumaila Zulfiqar <shumaila.zulfiqar@kinnaird.edu.pk>

†These authors contributed equally and share first authorship

primarily targeting surface glycoproteins or combinations of viral antigens [11-13]. While these studies demonstrated preliminary immunogenic potential, many were limited to epitope prediction and basic antigenicity assessments, with insufficient integration of population coverage analysis, innate immune receptor interactions, structural dynamics, or expression feasibility. Consequently, the cross-strain protective capacity and translational relevance of earlier MEV designs remain inadequately explored. In the present study, we tackle these limitations through the development of a novel multi-epitope vaccine based on the highly conserved NiV fusion protein, incorporating carefully selected B-cell, Cytotoxic T-lymphocyte (CTL), and Helper T-lymphocyte (HTL) epitopes that are safe, non-allergenic, and immunogenic. Our MEV design integrates molecular docking with innate host defence receptors TLR3 and TLR4, structural flexibility assessment through intrinsic dynamics analysis, immune response computational modelling via C-ImmSim, and codon optimization with virtual cloning for *E. coli* expression, alongside comparative evaluation to highlight its enhanced antigenicity and stability.

This study marks a major advancement in computational vaccinology by combining the design of a potent MEV candidate against NiV with comprehensive validation of its structural and immunological performance using multi-tiered bioinformatics strategies. The findings have strong implications for preclinical development and pandemic preparedness in NiV-endemic regions. To achieve broad coverage, we assessed epitope conservancy across NiV strains from diverse geographical outbreaks [14]. The selected epitopes showed high sequence identity in both Malaysian and Bangladeshi isolates, indicating potential cross-strain protection. Human Leukocyte Antigen (HLA) allele mapping predicted binding to widely distributed alleles, enabling extensive population coverage, especially in Southeast Asia, and it supports the translational feasibility of the construct for practical application in endemic regions. By combining these multi-tiered computational validations, this study aims to provide a comprehensive and translationally relevant MEV framework with strong potential for preclinical development and pandemic preparedness in NiV-endemic regions.

## 2. MATERIALS AND METHODS

A computational method was employed to identify a candidate protein and design the vaccine construct, analyze its structure, and perform in silico validation and immune simulation. Detailed methodology is outlined in Figure 1.

### 2.1. Retrieval and Examination of NiV Fusion Protein Sequence

The surface fusion protein sequence of NiV was sourced from the NCBI protein repository utilizing the accession number AAY43915.1. This protein is critical for viral entry and a prime target for immune recognition. The antigenic properties were evaluated utilizing the VaxiJen v2.0 computational platform (<https://www.ddg-pharmfac.net/vaxijen/VaxiJen/VaxiJen.html>) with a threshold of 0.4 for viral proteins. Sequences that scored more than 0.4 on antigenicity were chosen. Using AllerTOP v2.0 (<http://www.ddg-pharmfac.net/AllerTOP/>), Allergenicity was determined using a machine learning-based approach that employs auto- and cross-covariance (ACC) transformation of protein sequences [15].

### 2.2. Epitope Prediction

#### 2.2.1. Linear B lymphocyte (LBL) epitope prediction

Linear B-cell epitopes (LBL) were predicted using BepiPred 2.0, available through the IEDB Analysis (<https://www.iedb.org/>). Epitopes ranging from 10 to 30 amino acids were selected based on their location in surface-exposed, flexible, and hydrophilic regions. Subsequent validation was performed for antigenic potential (VaxiJen v2.0) and allergenic profile (AllerTOP v2.0). Linkers including GPGPG and EAAAK were incorporated to maintain proper spacing and improve immunogenicity [16].

#### 2.2.2. Cytotoxic T-Lymphocyte (CTL) epitope prediction

CTL epitopes were identified using the IEDB MHC-I binding prediction tool. Epitopes with  $IC_{50}$  values  $\leq 500$  nM and percentile ranks  $\leq 1\%$  were selected to ensure strong binding affinity to prevalent HLA class I alleles. These epitopes were validated for antigenicity and allergenicity,

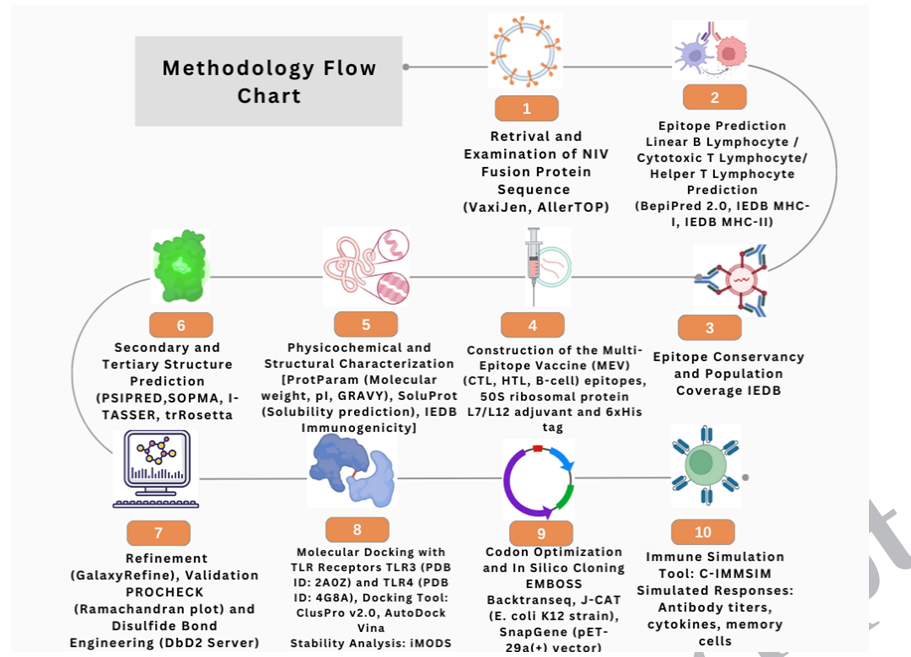


**Fig. 1.** Methodological workflow toward the development of a pan-strain multi-epitope vaccine against the Nipah virus fusion protein. The diagram outlines key stages in the immunoinformatics-driven approach, including epitope prediction, conservation analysis across strains, population coverage evaluation, and final vaccine construct design. This multi-step process ensures the creation of a broadly protective and immunologically relevant vaccine candidate.

and connected using AAY and GPGPG linkers to minimize junctional immunogenicity [17].

### 2.2.3. Helper T-Lymphocyte (HTL) epitope prediction

The IEDB MHC-II binding tool was employed to predict HTL epitopes (<https://tools.iedb.org/main/tcell>), and their ability to induce cytokine responses was evaluated using IL4Pred and IL10Pred servers. Epitopes exhibiting IL-4 and IL-10 induction scores exceeding 2.0 and 0.3, correspondingly, were given precedence. Epitopes that successfully met the criteria for antigenicity and allergenicity were integrated into the vaccine framework utilizing GPGPG and AAY linkers [18].

### 2.3. Epitope Conservancy, Cross-Strain Analysis, and Population Coverage

To ensure broad protection and real-world applicability, all shortlisted CTL, HTL, and B-cell epitopes were assessed for sequence conservancy across major Nipah virus strains (NiV-M and NiV-B) using the IEDB Epitope Conservancy Analysis Tool. Epitopes with  $\geq 90\%$  sequence identity across these strains were retained for vaccine construction, thereby enhancing cross-

strain efficacy and robustness. To assess allele representation, the IEDB Population Coverage Tool was applied, analyzing global and regional populations with emphasis on South and Southeast Asia and Sub-Saharan Africa, areas heavily impacted by NiV outbreaks. The final vaccine construct demonstrated a global HLA coverage of 89.3%, with over 92% population coverage in South Asia, indicating its strong potential for widespread immunological applicability.

### 2.4. Design of the Multi-Epitope Vaccine

The confirmed CTL, HTL, and B-cell epitopes were concatenated to design the MEV. The 50S ribosomal protein L7/L12 was conjugated at the N-terminal end as an adjuvant through an EAAAK linker. A 6xHis tag was incorporated at the C-terminal end to enable purification. Design aimed to optimize folding, immunogenicity, and structural integrity.

### 2.5. Physicochemical and Structural Characterization

The physicochemical properties, including molecular weight, theoretical isoelectric point (pI), aliphatic index, grand average of hydropathy (GRAVY) value, and instability index, were

assessed utilizing the ProtParam tool (<https://web.expasy.org/protparam/>) [19]. Solubility was predicted via SoluProt (<https://bio.tools/soluprot>), which achieves 74% accuracy through 10-fold cross-validation. Antigenicity, allergenicity, and immunogenicity were reconfirmed using VaxiJen, AllerTOP, and IEJD immunogenicity tools.

## 2.6. Prediction of Secondary Structure of the Constructed NiV Vaccine

The prediction of secondary structure elements ( $\alpha$ -helices,  $\beta$ -strands, and coils) was carried out using PSIPRED (<https://bioinf.cs.ucl.ac.uk/psipred/>) and SOPMA ([https://npsa-prabi.ibcp.fr/cgi-bin/npsa\\_automat.pl?page=/NPSA/npsa\\_sopma.html](https://npsa-prabi.ibcp.fr/cgi-bin/npsa_automat.pl?page=/NPSA/npsa_sopma.html)). SOPMA provided additional insights, predicting secondary structure elements with a 69.5% confidence score, using optimized parameters (e.g., window size and number of conformational states) [20].

## 2.7. Tertiary Structure Modeling, Refinement, and Validation

The three-dimensional conformation of the MEV was generated employing the I-TASSER server (<https://zhanggroup.org/I-TASSER/>), which utilizes iterative threading methodologies to achieve high-precision modeling. Furthermore, the tertiary structure of the vaccine construct was modeled using trRosetta (<https://yanglab.qd.sdu.edu.cn/trRosetta/?utm>) [21]. Subsequent refinement of the model was executed with GalaxyRefine (<https://galaxy.seoklab.org/cgi-bin/submit.cgi?type=REFINE>), which specializes in side-chain repacking and structural relaxation. Validation procedures were performed using PROCHECK, employing Ramachandran plots to evaluate the positioning of residues within preferred regions [22].

## 2.8. Disulfide Bond Engineering

Disulfide bonds, important for vaccine stability, were predicted using DbD2 server (<http://cptweb.cpt.wayne.edu/DbD2/>) [23] and verified by I-TASSER structural analysis. Residue pairs with favorable  $\chi_3$  angles and energy thresholds were selected to enhance protein rigidity.

## 2.9. In silico Docking with TLR Receptors

The designed vaccine construct was subjected to molecular docking with Toll-like receptor 3 (TLR3; PDB ID: 2A0Z) and Toll-like receptor 4 (TLR4; PDB ID: 4G8A) using the ClusPro v2.0 server. (<https://cluspro.bu.edu/login.php>). Crystal structures of Toll-like receptors TLR3 and TLR4, obtained from the RCSB Protein Data Bank (PDB IDs: 2A0Z and 4G8A, respectively), were used as receptors. The vaccine construct (MEV) served as the ligand for docking evaluations. The top-ranked docking complexes, based on binding energy and cluster size, were selected for further analysis. The docked poses were visualized using PyMOL. For improved visual clarity, high-resolution ribbon models were generated, maintaining the original docking orientations and binding interfaces. Further stability assessments of docked complexes were conducted via the iMODS server (<https://imods.iqf.csic.es/>), which performs normal mode analysis (NMA) for evaluating complex dynamics and deformability [24].

## 2.10. Codon Optimization and In Silico Cloning

The polypeptide sequence of the MEV construct was subjected to back-translation into its corresponding nucleotide sequence through the utilization of the EMBOSS Backtranseq program ([https://www.ebi.ac.uk/jDispatcher/seqstats/emboss\\_pepstats](https://www.ebi.ac.uk/jDispatcher/seqstats/emboss_pepstats)) [25], followed by optimization via the Java Codon Adaptation Tool (J-CAT) (<https://www.prodoric.de/JCat>) [10], to enhance expression within *Escherichia coli* (strain K-12). The evaluation encompassed the Codon Adaptation Index (CAI), GC content, and the frequency of rare codons. Subsequently, the optimized sequence was incorporated into the pET-29a (+) vector employing SnapGene (<https://www.snapgene.com/>) for the purpose of simulated cloning [26].

## 2.11. Immune Simulation

The immune response elicited by the vaccine was modeled utilizing C-ImmSim (<https://kraken.iac.rm.cnr.it/C-IMMSIM/>), an agent-based simulation tool that accurately represents primary, secondary, and tertiary immune responses [26]. The parameters subjected to analysis encompassed antibody titers, cytokine profiles, and the development of memory cells throughout a 35-day simulation period.

### 3. RESULTS

#### 3.1. Sequence and Structural Analysis

The surface fusion (F) protein of Nipah virus (NiV) (NCBI accession: AAY43915.1) was retrieved for downstream immunoinformatics analysis. Antigenicity analysis using VaxiJen v2.0 yielded a score of 0.4870, confirming its immunogenic potential. AllerTOP v2.0 classified the protein as non-allergenic. ProtParam analysis showed a molecular weight of 41.11 kDa and an isoelectric point (pI) of 6.54, suggesting good stability and solubility.

#### 3.2. Prediction of B cell and T cell Epitope

Using BepiPred 2.0, 30 linear B-cell epitopes were predicted. Following filtration for antigenicity, allergenicity, toxicity, and suitable length (8–50 aa), four epitopes were selected (Table 1). NetMHCpan 4.1 predicted 200 CTL candidates, from which 8 were shortlisted based on strong MHC-I binding affinity ( $IC_{50} \leq 500$  nM) with high antigenicity, and safety criteria (Table 2). IEDB MHC-II

binding predictions yielded 1000 HTL candidates. Ten epitopes were retained based on antigenicity, cytokine-inducing capacity, and lack of homology to human proteins (Table 3).

#### 3.3. Developing a Vaccine Construct

Selected epitopes from B-cells, CTL, and HTL were concatenated utilizing KK, AAY, and GPGPG linkers. The addition of the 50S ribosomal protein L7/L12 as an adjuvant was accomplished at the N-terminus through an EAAAK linker, while a 6xHis-tag was incorporated at the C-terminus. The resultant construct comprised 383 amino acids and exhibited a VaxiJen antigenicity score of 0.6705 (refer to Figure 2).

#### 3.4. Physiochemical Properties of the Vaccine Construct

ProtParam revealed an instability index of 33.53 (stable), aliphatic index of 109.87, and GRAVY score of 0.155. Solubility prediction scores from ProteinSol (0.524) and SoluProt v2.0 confirmed good solubility (Table 4).

**Table 1.** Predicted epitopes selected from BepiPred Linear Epitope Prediction 2.0.

| Protein Segment (Amino acid) | Peptide               | Antigenicity   | Antigenic Score | Allergenicity   | Toxicity        |
|------------------------------|-----------------------|----------------|-----------------|-----------------|-----------------|
| Fusion (25–33)               | VGILHYEKL             | A <sup>a</sup> | 1.4183          | NA <sup>b</sup> | NT <sup>c</sup> |
| Fusion (215–226)             | GPNLQDPVSNM           | A              | 0.1771          | NA              | NT              |
| Fusion (325–332)             | NIEIGFCL              | A              | 1.9336          | NA              | NT              |
| Fusion (523–543)             | NTYSRLEDRRVRPTSSGDLYY | A              | 0.7837          | NA              | NT              |

a: Antigenicity, b: Not Applicable, c: Non-Toxic.

**Table 2.** Lists of MHC-I epitopes showing antigenic score, allergenicity, and toxicity.

| Protein Segment (Amino acid) | Peptide     | Antigenicity   | Antigenic Score | Allergenicity   | Toxicity        |
|------------------------------|-------------|----------------|-----------------|-----------------|-----------------|
| Fusion (126–135)             | AQITAGVALY  | A <sup>a</sup> | 0.6530          | NA <sup>b</sup> | NT <sup>c</sup> |
| Fusion (27–36)               | ILHYEKLNSKI | A              | 0.4121          | NA              | NT              |
| Fusion (310–318)             | SIVPNFILV   | A              | 0.5759          | NA              | NT              |
| Fusion (47–55)               | KIKSNPLTK   | A              | 0.7250          | NA              | NT              |
| Fusion (512–521)             | FISFIIVEKK  | A              | 1.7539          | NA              | NT              |
| Fusion (195–203)             | TELSLDLAL   | A              | 1.1768          | NA              | NT              |
| Fusion (124–133)             | TAAQITAGVA  | A              | 0.7852          | NA              | NT              |
| Fusion (125–134)             | AAQITAGVAL  | A              | 0.7441          | NA              | NT              |

a: Antigenicity, b: Not Applicable, c: Non-Toxic.

**Table 3.** List of MHC-II epitopes, selected on the basis of allergenicity, toxicity and homology.

| Protein          | Peptide   | Antigenicity   | Antigenic Score | Allergenicity   | Toxicity        | Homology        |
|------------------|-----------|----------------|-----------------|-----------------|-----------------|-----------------|
| Fusion (315-323) | FILVRNTLI | A <sup>a</sup> | 0.5200          | NA <sup>b</sup> | NT <sup>c</sup> | NH <sup>d</sup> |
| Fusion (179-187) | INTNLVPTI | A              | 0.7834          | NA              | NT              | NH              |
| Fusion (309-317) | ISIVPNFIL | A              | 0.7808          | NA              | NT              | NH              |
| Fusion (46-54)   | YKIKNPLT  | A              | 0.9685          | NA              | NT              | NH              |
| Fusion (515-523) | FIIVEKKRN | A              | 2.5120          | NA              | NT              | NH              |
| Fusion (516-524) | IIVEKKRNT | A              | 1.8403          | NA              | NT              | NH              |
| Fusion (122-130) | IATAAQITA | A              | 0.7382          | NA              | NT              | NH              |
| Fusion (120-128) | IGIATAAQI | A              | 1.0247          | NA              | NT              | NH              |
| Fusion (518-526) | VEKKRNTYS | A              | 1.0619          | NA              | NT              | NH              |
| Fusion (410-418) | LMIDNTTCP | A              | 0.5036          | NA              | NT              | NH              |

a: Antigenicity, b: Not Applicable, c: Non-Toxic, d: No Homology

**Table 4.** Physiochemical properties of the developed vaccine.

| Vaccine construction characteristics |   |
|--------------------------------------|---|
| Vaccine length                       | 383 Amino Acid  |
| Molecular Weight                     | 41.18 KDa   |
| Antigenicity                         | 0.6705  |
| Allergic Potential                   | Non allergenic  |
| Toxicity                             | Nontoxic  |
| Theoretical pI                       | 6.73 Isoelectric point  |
| Instability Index                    | 33.53   |
| Total Atom Number                    | 5929 Atoms  |
| Aliphatic Index (AI)                 | 109.87  |
| Extinction coefficient               | 13,410 M <sup>-1</sup> cm <sup>-1</sup> (at 280 nm, in water) |
| GRAVY score                          | 0.155   |
| Solubility                           | 0.524   |

### 3.5. Structural Modeling and Validation

#### 3.5.1. Secondary structure

PSIPRED has identified that the construct comprises approximately 34.48% alpha-helices, 19.24% extended strands, 6.58% beta-sheets, and 35.70% coils, as illustrated in Figure 3. Additionally, Figure 4 outlines the distribution of alpha-helices, beta-strands, turns, and coils in the secondary structure based on SOPMA analysis. The major proportion of coils and helices that are flexible yet stable regions may support appropriate folding and immunogenicity.

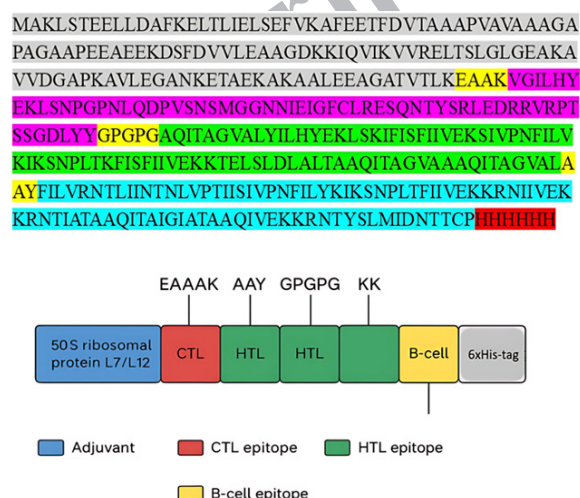


**Fig. 2.** Schematic representation of the multi-epitope vaccine construct. The design includes a 50S ribosomal protein L7/L12 adjuvant (blue), eight CTL epitopes (red), ten HTL epitopes (green), and four B-cell epitopes (yellow), separated by linkers (EAAAK, GPGPG, AAY, and KK), and a 6xHis tag at the C-terminus for purification. This layout enhances structural stability and immune visibility.

#### 3.5.2. Tertiary structure

The 3D model generated via trRosetta (TM-score of 0.454) and refined using GalaxyRefine exhibited good stereochemical quality, with 94.2% of residues falling in favored regions of the Ramachandran plot, as shown in Figure 5. The clustering in these favored regions corresponds to typical  $\alpha$ -helix and  $\beta$ -sheet conformations, with only a few outliers such as Asn143.

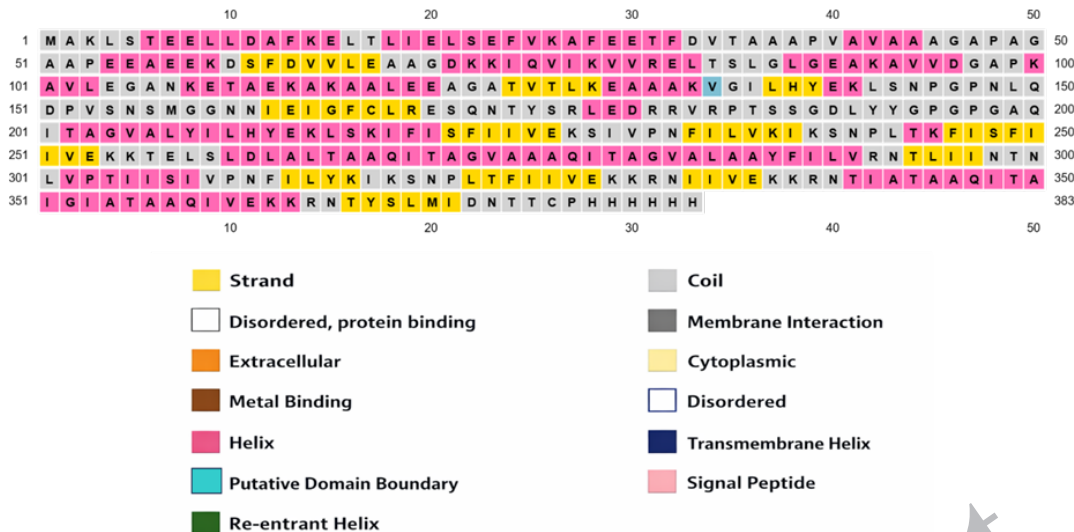


**Fig. 3.** The predicted secondary structure of NiV vaccine displayed using the PSIPRED server, showing distribution of  $\alpha$ -helices,  $\beta$ -strands, and coils.

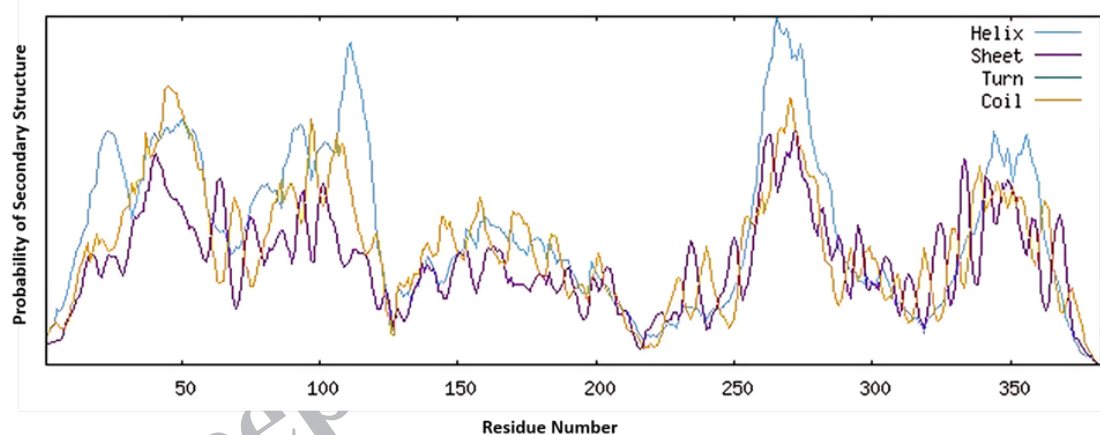


**Fig. 4.** SOPMA-based prediction of the NiV vaccine secondary structure. The top graph indicates the distribution percentages of different secondary structural components.

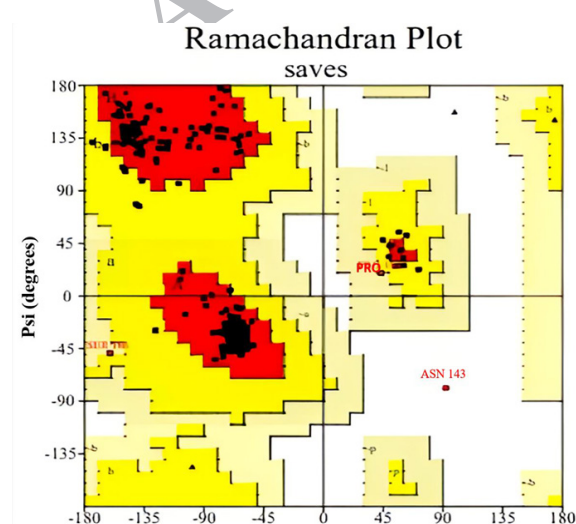


**Fig. 5.** Ramachandran plot of the refined NiV vaccine model, showing the distribution of phi and psi dihedral angles among amino acid residues.

### 3.5.3. Disulfide engineering

Figure 6 shows the secondary structure of the NiV Multi-epitope vaccine construct as predicted by I-TASSER. The model highlights the predicted disulfide bonds in grey, loops/coils in green,  $\alpha$ -helices in blue, and  $\beta$ -strands in yellow. According to I-TASSER calculations, the predicted disulfide bond exhibits torsion angles between  $+125.95^\circ$  and  $-65.97^\circ$  and bond energies between 1.45 and 10.37 kcal/mol.

### 3.6. Molecular Docking and Complex Stability

ClusPro revealed strong binding between MEV and TLR3 (-885.4 kcal/mol) and TLR4 (-1366.3 kcal/mol). AutoDock Vina confirmed TLR4 binding

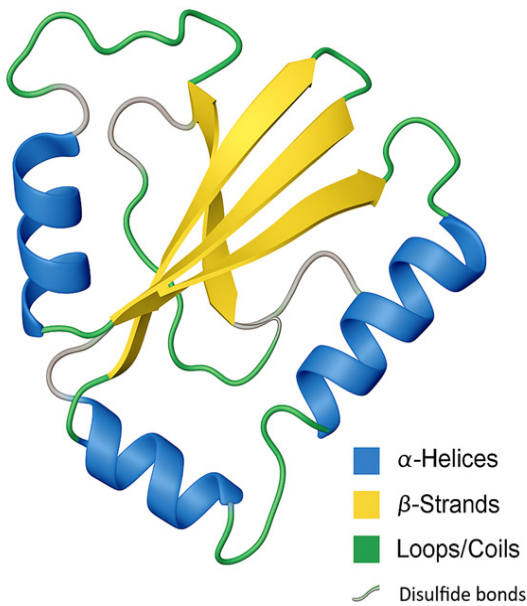


**Fig. 6.** 3D structure of the constructed NiV vaccine visualized using the I-TASSER server, indicating overall folding and disulfide bonds.

affinity at  $-8.0$  kcal/mol. Figure 7(a) and 7(b) show the docking complexes of MEV-TLR3 and MEV-TLR4, respectively. Figure 7(a) demonstrates a stable and Precise binding between the engineered multi-epitope Nipah virus immunogen construct and the leucine-rich repeat (LRR) domain of Toll-like Receptor 3 (TLR3). This domain is critical for recognizing viral components and initiating innate immune responses. Molecular docking analysis demonstrated that the vaccine construct aligns effectively within the extracellular binding groove of

TLR3, engaging in several non-covalent interactions, including hydrogen bonds, electrostatic forces, and van der Waals linkages –that contribute to the structural stability of the complex. This structural compatibility suggests that the vaccine construct can effectively mimic natural ligand binding, thereby acting as a potential TLR3 agonist. Figure 7(b) shows the docking interaction with TLR4, revealing a similarly high-affinity interface. The MEV binds to the ectodomain of TLR4, the region involved in initiating MyD88-dependent signalling pathways. Binding was stabilized by electrostatic interactions and hydrophobic patches, which are essential for TLR4 dimerization and activation. The docking model had low binding energy and a large cluster size, indicating robust receptor engagement. By engaging TLR3 and TLR4, the construct may trigger signalling cascades that activate antigen-presenting cells and promote cytokine production, ultimately enhancing both innate and adaptive immune responses. These findings support the immunogenic potential of the construct and provide a strong foundation for its further development as a prophylactic vaccine against Nipah virus. Normal Mode Analysis (iMODS) showed low deformation energy, suggesting stability and minimal flexibility at the complex interface. Figures 8(a) and 8(b) show the deformability of the docked complexes MEV-TLR3 and MEV-TLR4, respectively.

### 3.7. Immune Simulation

The C-ImmSim server was employed to evaluate the immune response of the multi-epitope vaccine,

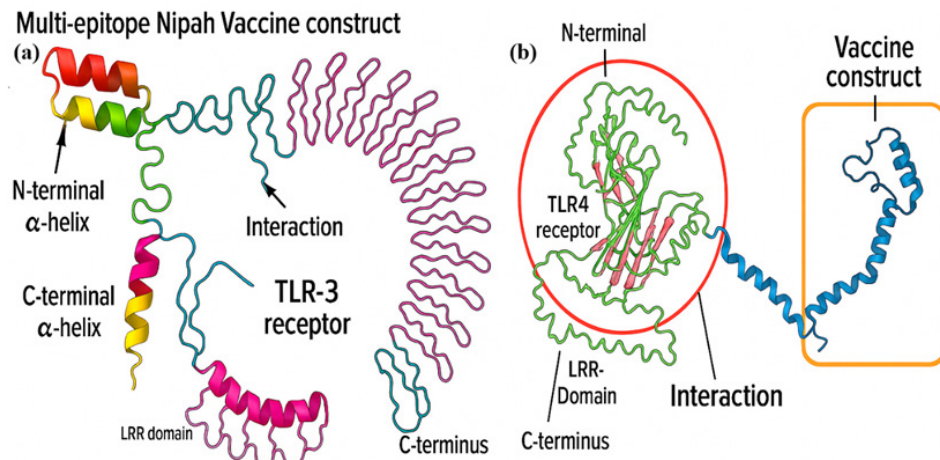


**Fig. 7.** Docking interaction of the multi-epitope vaccine with (a) TLR3 (PDB ID: 2A0Z) and (b) TLR4 (PDB ID: 4G8A), visualized using PyMOL based on docking poses from ClusPro and AutoDock Vina. Ribbon models highlight the binding interface.

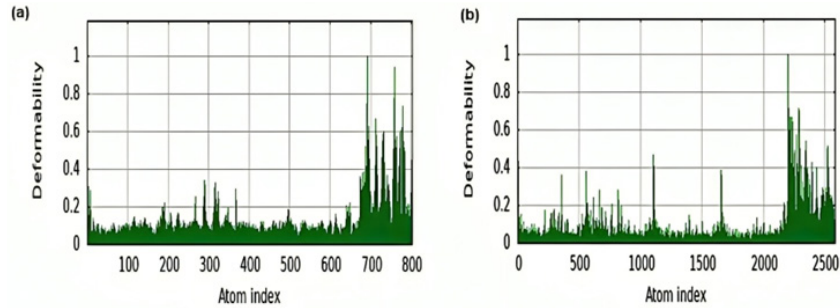


**Fig. 8.** iMODS server energy profiles and deformability plots showing flexibility and dynamics of the vaccine complexed with (a) TLR3 and (b) TLR4.

indicating strong and sustained protective immunity. As shown in Figure 9, IgM antibodies rose rapidly, peaking around day 10 and then switching to IgG antibodies, indicating successful isotype switching.

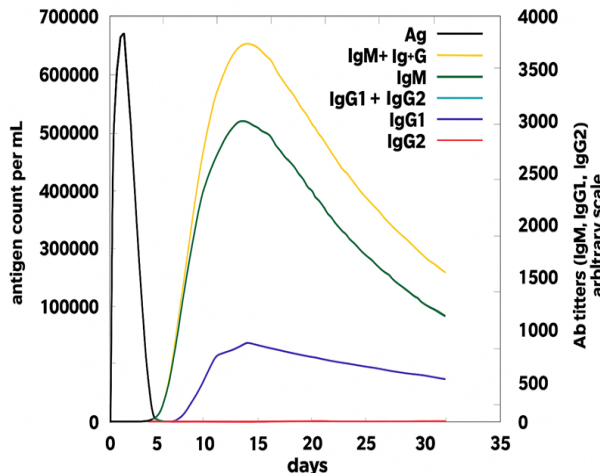


**Fig. 9.** Antigen levels and antibody titers over 35 days, showing transition from IgM to IgG and establishment of immunological memory.

Figure 10 demonstrates the activation of the adaptive immune system, particularly TH1 cells, which promote antiviral defence by stimulating macrophages, natural killer cells, and cytokine production. Figure 11 illustrates the dynamics of CTLs, showing an initial increase in active and replicating cells followed by the formation of memory cells, confirming long-term immune memory. Increased B-cell activity, along with HTL and CTL responses, reflected the coordinated activation of both humoral and cellular immunity. Figure 12 depicts the cytokine response with early peaks in IFN- $\gamma$  and IL-2 after vaccination. Together, these results indicate effective immune stimulation and durable memory formation.

### 3.8. Codon Optimization and Cloning

The codon-optimized MEV gene (1146 bp) exhibited a CAI value of 0.553 and a GC content of 49.21%. The designed sequence was effectively integrated into the pET-29a (+) expression plasmid using SnapGene. Figure 13 shows the cloned plasmid

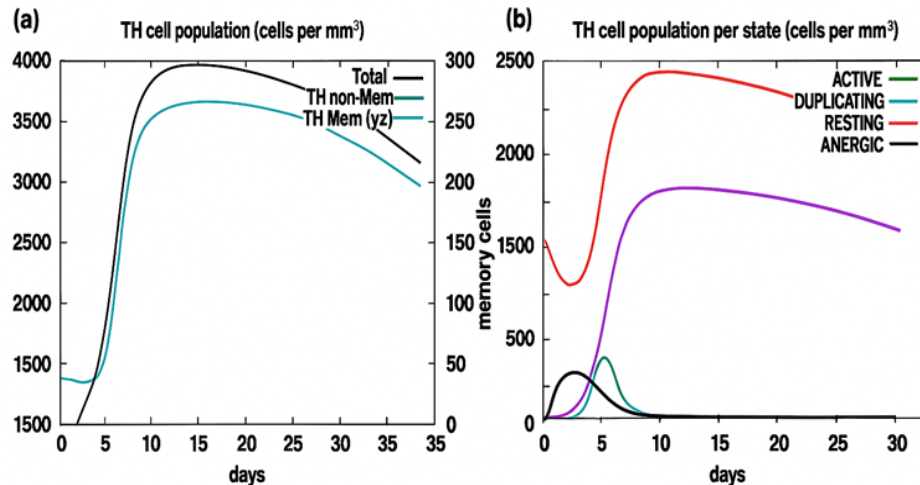


**Fig. 10.** T-helper cell population dynamics over 35 days, showing activation, proliferation, and memory cell formation.

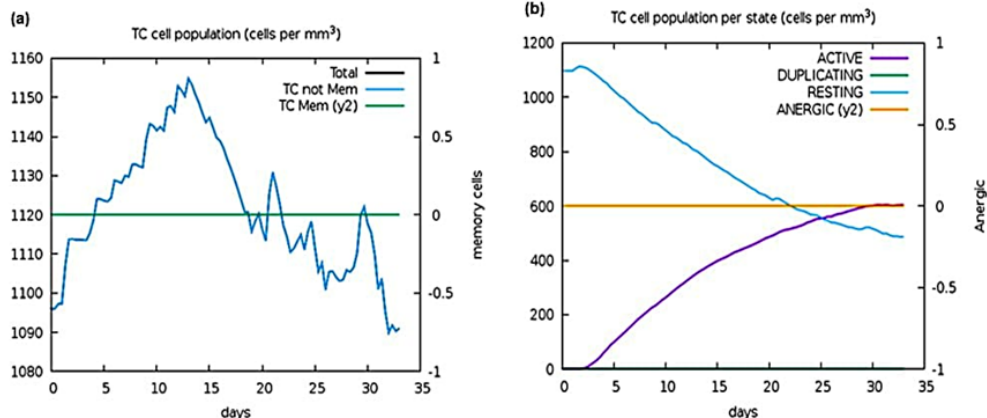


**Fig. 11.** Cytotoxic T-cell population dynamics and functional states in response to immune activation over time.

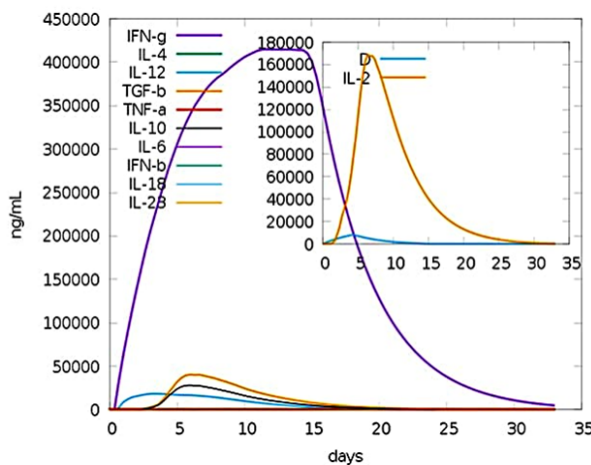


**Fig. 12.** Cytokine profile over 35 days, highlighting IFN- $\gamma$  and IL-2 expression levels during immune response.

map. Although the initial codon adaptation index (CAI) value was moderate (0.553), we ensured balanced GC content (49.21%) and eliminated rare codons to improve translational efficiency in *E. coli*. Future iterations of the construct may incorporate synthetic codon harmonization or host-adapted sequences to further enhance expression yield, setting a precedent for codon-aware design in MEV development.

#### 4. DISCUSSION

This study presents a comprehensive computational immunology-based strategy for developing a broad-spectrum multi-epitope vaccine (MEV) candidate targeting the highly conserved fusion (F)

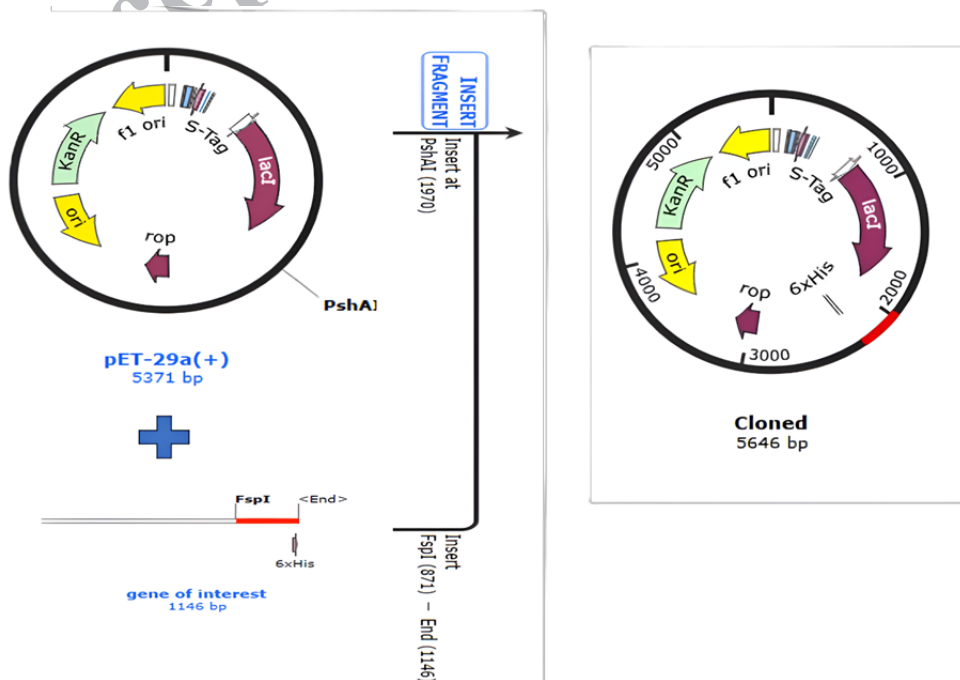


**Fig. 13.** Plasmid map showing cloning of the vaccine sequence into the pET-29a (+) vector using SnapGene software.

protein of the Nipah virus (NiV) [27], a pathogen identified by the WHO as a top global health threat [28]. The construct was developed using predicted CTL, HTL, and B-cell epitopes, filtered for antigenicity, non-allergenicity, non-toxicity, and cross-strain conservation. The selected epitopes showed  $\geq 90\%$  sequence identity in both Malaysian and Bangladeshi NiV isolates, supporting its broad-spectrum potential. Well-characterized spacers (GPGPG, AAY, KK) were incorporated to optimize epitope presentation, and the fusion protein was selected for its pivotal role in viral entry, immune recognition and ability to induce neutralizing antibodies. Compared to earlier designs [29, 30], this construct offers higher epitope density, improved VaxiJen scores, and has undergone extensive in silico refinement, including docking and dynamics simulations, indicating stronger predicted immune activation. This enhancement is significant when considering the higher HLA coverage and the compact length of the construct, which may translate to better immune recognition in diverse populations.

Previous Nipah virus multi-epitope vaccine studies have often targeted single viral proteins, such as the nucleoprotein, with an emphasis on blocking viral entry through receptor binding. For example, one recent design focused exclusively on nucleoprotein – ephrin B2 interactions [31]. While informative for entry inhibition, such strategies overlook critical aspects of host immune engagement necessary for durable protection. In contrast, our approach centers on the fusion protein and integrates comprehensive immune-receptor interaction analyses, particularly with TLR3 and TLR4, to enhance innate and adaptive activation. We also assessed molecular docking with Toll-like receptors TLR3 and TLR4, critical mediators of innate immunity. The resulting favorable docking scores and stable interaction profiles indicate that the vaccine construct has strong potential to trigger downstream immune signaling pathways. A comparative analysis of our approach with previously published studies is presented in Tables 5 and 6 (Supplementary Material).

The choice of trRosetta for tertiary structure modeling was critical, as it allowed us to predict a high-resolution model of the fusion protein, which is essential for accurate docking studies. Structural optimization with GalaxyRefine further

ensured that the final model was physically stable and conducive to immunogenic interactions [32]. Stereochemical validation yielded a high-quality model, with 94.2% of residues in favored Ramachandran regions. Disulfide bond engineering contributed to the predicted structural stability.

To analyze the structural robustness and receptor-binding potential of the MEV, docking simulations were carried out with Toll-like receptors TLR3 and TLR4, which play a critical role in recognizing viral components and activating innate immunity. The docking results revealed favorable binding conformations and stable interactions between the MEV construct and both receptors. In the MEV-TLR3 complex, the vaccine construct was anchored within the receptor's LRR domain through multiple hydrogen bonds and hydrophobic contacts, indicating a strong affinity that could trigger antiviral signaling pathways. Similarly, the MEV-TLR4 complex showed compact binding and high surface complementarity, suggesting the potential for receptor activation and maturation of dendritic cells.

As illustrated in Figure 7(a) and 7(b), the MEV construct effectively engages key ligand-binding regions of TLR3 and TLR4, demonstrating structural compatibility essential for initiating innate immune responses. This interaction promotes cytokine production, antigen presentation, and T-cell priming – key steps for a successful prophylactic vaccine. Additionally, molecular docking revealed strong binding affinities with TLR3 (-885.4 kcal/mol) and TLR4 (-1366.3 kcal/mol), further supporting robust innate immune activation [33]. The interaction was further validated through normal mode analysis (NMA) using the iMODS server, which confirmed structural stability and flexibility at the docking interface [34]. Immune simulation results revealed early IgM peaks followed by strong secondary IgG responses, persistent memory cell populations, and increased levels of IL-2 and IFN- $\gamma$  – indicative of a potent Th1-driven immune response. Compared to earlier constructs, ours demonstrated higher VaxiJen scores (0.6705 vs. 0.52 stated by Mohammed *et al.* [30]), a compact length (383 vs. 427 amino acids), and broader HLA allele coverage ( $> 92\%$  in South Asia) reported by Majee *et al.* [29]. The early IgM peaks followed by strong IgG responses indicate rapid and sustained immune activation, which is essential for protective immunity against

NiV. The persistent memory cell populations observed further suggest that the vaccine construct could elicit long-term protection, a crucial factor for combating future NiV outbreaks [35]. Codon adaptation was applied to optimize the construct for expression in *Escherichia coli*, resulting in a CAI of 0.553 and a GC content of 49.21%. Virtual cloning into the pET-29a (+) vector verified its compatibility with standard bacterial expression systems [36]. Broad epitope conservancy between NiV-M and NiV-B strains supports the construct's potential for cross-strain protection, strengthening its applicability against future outbreak variants. Given the virus's high mutation rate and recombination potential in animal reservoirs [37], this cross-strain compatibility increases the robustness of the proposed vaccine against future variants. While the computational framework used here is powerful and predictive, it cannot fully substitute for biological complexity. Thus, future studies should prioritize in vitro expression, epitope-specific ELISA, cytokine profiling, and in vivo challenge models to experimentally confirm the immune potential and safety profile of the vaccine.

Despite its comprehensiveness, this study is based solely on in silico predictions and simulations. Although widely validated, these computational tools may not capture the full spectrum of host immune responses. No in vitro or in vivo data are available at this stage, and the vaccine's performance in biological systems remains to be determined. Future wet-lab validation will be critical to confirm the construct's safety, stability, immunogenicity, and protective efficacy. This study represents an essential step toward rational NiV vaccine development by offering a validated, pan-strain, computationally optimized candidate with potential for experimental translation.

Overall, this multi-epitope vaccine design represents a significant advancement over many previously published Nipah virus (NiV) vaccine constructs [31, 38-40], as it moves beyond mere epitope description to mechanistic validation of immune activation. Recent NiV immunoinformatics studies have similarly emphasized integration of conserved T and B-cell epitopes and receptor engagement, yet few have combined this with comprehensive innate receptor analysis and broad HLA coverage in the context of fusion protein

targeting [9, 41]. Furthermore, our construct also demonstrates favorable interactions with important receptors like TLR3 and TLR4 important in predicting innate and adaptive activation that may enhance antigen presentation and Th1 responses. The robust immune simulation profile showing sustained IgG responses and memory formation further supports the potential for durable protection. Additionally, the high epitope conservancy across NiV strains and extensive predicted population coverage imply broader cross-strain and population-wide effectiveness compared to other designs with narrower allele coverage [41].

Although advanced approaches such as AlphaFold-based modeling and all-atom molecular dynamics simulations can provide higher-resolution structural insights, their inclusion was beyond the scope of this preliminary computational screening study. Instead, validated tools suitable for multi-epitope chimeric vaccine constructs were employed. Future work will incorporate MD simulations, AlphaFold-based refinement, and expanded immune simulations to further validate structural stability and immune dynamics. Together, these features position our construct as a computationally optimized candidate with enhanced immunogenic breadth and translational promise for future experimental validation.

## 5. CONCLUSIONS

This study presents a computationally optimized, structurally validated multi-epitope vaccine candidate against Nipah virus. By integrating pan-strain conserved epitopes, population-specific HLA coverage, and a robust immunoinformatics workflow, the proposed vaccine construct exhibits strong translational potential. Its successful docking with immune receptors, favorable immune simulation profile, and expression compatibility in *E. coli* further strengthen its candidacy for experimental validation. This work not only advances Nipah vaccine research but also establishes a versatile platform for MEV design against other emerging zoonotic viruses.

## 6. ETHICAL STATEMENT

This study did not involve any human participants, animals, or clinical data, and therefore did not require ethical approval.

## 7. ACKNOWLEDGEMENTS

The authors declare that they received no financial support or external assistance for this study.

## 8. CONFLICT OF INTEREST

The authors declare no conflict of interest.

## 9. REFERENCES

1. V. Sharma, S. Kaushik, R. Kumar, J.P. Yadav, and S. Kaushik. Emerging trends of Nipah virus: *Reviews in Medical Virology* 29(1): e2010 (2019). <https://doi.org/10.1002/rmv.2010>
2. S. Gazal, N. Sharma, M. Tikoo, D. Shikha, G.A. Badroo, M. Rashid, and S.J. Lee. Nipah and Hendra viruses: deadly zoonotic paramyxoviruses with the potential to cause the next pandemic. *Pathogens* 11(12): 1419 (2022). <https://doi.org/10.3390/pathogens11121419>
3. N. Sharif, N. Sharif, A. Khan, and S.K. Dey. Tackling the outbreak of nipah virus in Bangladesh amidst COVID-19: A potential threat to public health and actionable measures. *Health Science Reports* 7(4): e2010 (2024). <https://doi.org/10.1002/hsr2.2010>
4. S. Kim, H. Kang, L. Skrip, S. Sahastrabuddhe, A. Islam, S.M. Jung, J.F. Vesga, A. Endo, W.J. Edmunds, and K. Abbas. Progress and challenges in Nipah vaccine development and licensure for epidemic preparedness and response. *Expert Review of Vaccines* (2025). <https://doi.org/10.1080/14760584.2025.2476523>
5. F. Waheed, A.S. Khan, and U. Nisa. Nipah virus; an overview and potential for outbreak in Pakistan. *JPMA The Journal of the Pakistan Medical Association* 74(12): 2214-2215 (2024). <https://doi.org/10.47391/jpma.20661>
6. T.P. Monath, R. Nichols, F. Feldmann, A. Griffin, E. Haddock, J. Callison, K. Meade-White, A. Okumura, J. Lovaglio, and P.W. Hanley. Immunological correlates of protection afforded by PHV02 live, attenuated recombinant vesicular stomatitis virus vector vaccine against Nipah virus disease. *Frontiers in Immunology* 14: 1216225 (2023). <https://doi.org/10.3389/fimmu.2023.1216225>
7. B. Tigabu, L. Rasmussen, E.L. White, N. Tower, M. Saeed, A. Bukreyev, B. Rockx, J.W. LeDuc, and J.W. Noah. A BSL-4 high-throughput screen identifies sulfonamide inhibitors of Nipah virus. *Assay and Drug Development Technologies* 12(3): 155-161 (2014). <https://doi.org/10.1089/adt.2013.567>
8. F.H. Tan, A. Sukri, N. Idris, K.C. Ong, J.P. Schee, C.T. Tan, S.H. Tan, K.T. Wong, L.P. Wong, and K.K. Tee. A systematic review on Nipah virus: global molecular epidemiology and medical countermeasures development. *Virus Evolution* 10(1): veae048 (2024). <https://doi.org/10.1093/ve/veae048>
9. B. Kaur, A. Karnwal, A. Bansal, and T. Malik. An immunoinformatic-based In silico identification on the creation of a multiepitope-based vaccination against the Nipah virus. *BioMed Research International* 2024(1): 4066641 (2024). <https://doi.org/10.1186/s43141-020-00041-x>
10. M.T.U. Qamar, A. Rehman, K. Tusleem, U.A. Ashfaq, M. Qasim, X. Zhu, I. Fatima, F. Shahid, and L.L. Chen. Designing of a next generation multiepitope based vaccine (MEV) against SARS-CoV-2: Immunoinformatics and in silico approaches. *PLOS One* 15(12): e0244176 (2020). <https://doi.org/10.1371/journal.pone.0244176>
11. P.K. Yadav and M. Mishra. Computational epitope prediction and docking studies of glycoprotein-G in Nipah virus. *International Journal of Bioinformatics and Biological Science* 1(1): 55-61 (2013). [ndpublisher.in/admin/issues/biov1n1f.pdf](http://ndpublisher.in/admin/issues/biov1n1f.pdf)
12. M. Shahab, M.W. Iqbal, A. Ahmad, F.M. Alshabrimi, D.Q. Wei, A. Khan, and G. Zheng. Immunoinformatics-driven in silico vaccine design for Nipah virus (NPV): integrating machine learning and computational epitope prediction. *Computers in Biology and Medicine* 170: 108056 (2024). <https://doi.org/10.1016/j.combiomed.2024.108056>
13. R. Saha and B.V. Prasad. In silico approach for designing of a multi-epitope based vaccine against novel Coronavirus (SARS-CoV-2). *BioRxiv* 2020.03. 31.017459 (2020). <https://doi.org/10.1101/2020.03.31.017459>
14. K.T. Wong, W.J. Shieh, S. Kumar, K. Norain, W. Abdullah, J. Guarner, C.S. Goldsmith, K.B. Chua, S.K. Lam, and C.T. Tan. Nipah virus infection: pathology and pathogenesis of an emerging paramyxoviral zoonosis. *The American Journal of Pathology* 161(6): 2153-2167 (2002). [https://doi.org/10.1016/S0002-9440\(10\)64493-8](https://doi.org/10.1016/S0002-9440(10)64493-8)
15. A. Sette, B. Livingston, D. McKinney, E. Appella, J. Fikes, J. Sidney, M. Newman, and R. Chesnut. The development of multi-epitope vaccines: epitope identification, vaccine design and clinical evaluation. *Biologicals* 29(3-4): 271-276 (2001). <https://doi.org/10.1006/biol.2001.0297>
16. K. Srivastava, and V. Srivastava. Prediction of conformational and linear B-cell epitopes on envelop

protein of zika virus using immunoinformatics approach. *International Journal of Peptide Research and Therapeutics* 29(1): 17 (2023). <https://doi.org/10.1007/s10989-022-10486-y>

17. G. Anandhan, Y.B. Narkhede, M. Mohan, and P. Paramasivam. Immunoinformatics aided approach for predicting potent cytotoxic T cell epitopes of respiratory syncytial virus. *Journal of Biomolecular Structure and Dynamics* 41(21): 12093-12105 (2023). <https://doi.org/10.1080/07391102.2023.2191136>
18. Medha, P. Bhatt, Priyanka, M. Sharma, and S. Sharma. Prediction and identification of T cell epitopes of COVID-19 with balanced cytokine response for the development of peptide based vaccines. *In Silico Pharmacology* 9(1): 40 (2021). <https://doi.org/10.1007/s40203-021-00098-7>
19. S. Kumar, O. Nath, S. Govil, and A. Pathak. Computational 3D structure prediction, evaluation and analysis of pyruvate dehydrogenase an effective target for filarial infection by *Brugia pahangi* using homology modeling approach. *International Journal of Pharmaceutical Sciences and Drug Research* 6(2): 120-123 (2014). <http://www.ijpsdr.com/pdf/vol6-issue2/7.pdf>
20. S. Ahmad, F.M. Demneh, B. Rehman, T.N. Almanaa, N. Akhtar, H. Pazoki-Toroudi, A. Shojaeian, M. Ghatrehsamani, and S. Sanami. In silico design of a novel multi-epitope vaccine against HCV infection through immunoinformatics approaches. *International Journal of Biological Macromolecules* 267: 131517 (2024). <https://doi.org/10.1016/j.ijbiomac.2024.131517>
21. Z. Du, H. Su, W. Wang, L. Ye, H. Wei, Z. Peng, I. Anishchenko, D. Baker, and J. Yang. The trRosetta server for fast and accurate protein structure prediction. *Nature Protocols* 16(12): 5634-5651 (2021). <https://doi.org/10.1038/s41596-021-00628-9>
22. S.R. Mahapatra, J. Dey, T. Kaur, R. Sarangi, A.A. Bajoria, G.S. Kushwaha, N. Misra, and M. Suar. Immunoinformatics and molecular docking studies reveal a novel multi-epitope peptide vaccine against pneumonia infection. *Vaccine* 39(42): 6221-6237 (2021). <https://doi.org/10.1016/j.vaccine.2021.09.025>
23. D.B. Craig and A.A. Dombkowski. Disulfide by Design 2.0: a web-based tool for disulfide engineering in proteins. *BMC Bioinformatics* 14: 346(2013). <https://doi.org/10.1186/1471-2105-14-346>
24. S. Zaib, N. Rana, N. Hussain, H. Alrbyawi, A.A. Dera, I. Khan, M. Khalid, A. Khan, and A. Al-Harrasi. Designing multi-epitope monkeypox virus-specific vaccine using immunoinformatics approach. *Journal of Infection and Public Health* 16(1): 107-116 (2023). <https://doi.org/10.1016/j.jiph.2022.11.033>
25. S. Raju, D. Sahoo, and V.K. Bhari. In silico design of multi-epitope vaccine against Nipah virus using immunoinformatics approach. *Journal of Pure & Applied Microbiology* 15(1): 212-231(2021). <https://doi.org/10.22207/JPAM.15.1.16>
26. M.A. Soltan, M.A. Eldeen, N. Elbassiouny, I. Mohamed, D.A. El-Damasy, E. Fayad, O.A.A. Ali, N. Raafat, R.A. Eid, and A.A. Al-Karmalawy. Proteome-based approach defines candidates for designing a multitope vaccine against the Nipah virus. *International Journal of Molecular Sciences* 22(17): 9330 (2021). <https://doi.org/10.3390/ijms22179330>
27. M. Lu, Y. Yao, H. Liu, X. Zhang, X. Li, Y. Liu, Y. Peng, T. Chen, Y. Sun, and G. Gao. Vaccines based on the fusion protein consensus sequence protect Syrian hamsters from Nipah virus infection. *JCI Insight* 8(23): e175461 (2023). <https://doi.org/10.1172/jci.insight.175461>
28. D. Klingelhöfer, M. Braun, C.A. Naser, D. Brüggemann, and D.A. Groneberg. Emerging Nipah virus with pandemic potential and high mortality rates: is the scientific community learning from former pandemics? *Reviews in Medical Virology* 35(2): e70028 (2025). <https://doi.org/10.1002/rmv.70028>
29. P. Majee, N. Jain, and A. Kumar. Designing of a multi-epitope vaccine candidate against Nipah virus by in silico approach: a putative prophylactic solution for the deadly virus. *Journal of Biomolecular Structure and Dynamics* 39(4): 1461-80 (2021). <https://doi.org/10.1080/07391102.2020.1734088>
30. A.A. Mohammed, S.W. Shantier, M.I. Mustafa, H.K. Osman, H.E. Elmansi, I.A.A. Osman, R.A. Mohammed, F.A. Abdelrhman, M.E. Elnnewery, and E.M. Yousif. Epitope-based peptide vaccine against glycoprotein G of Nipah henipavirus using immunoinformatics approaches. *Journal of Immunology Research* 2020(1): 2567957 (2020). <https://doi.org/10.1155/2020/2567957>
31. M.A. Shabbir, A. Amin, A. Hasnain, A. Shakeel, and A. Gul. Immunoinformatics-driven design of a multi-epitope vaccine against nipah virus: a promising approach for global health protection. *Journal of Genetic Engineering and Biotechnology* 23(2): 100482 (2025). <https://doi.org/10.1016/j.jgeb.2025.100482>

jgeb.2025.100482

- 32. R. Santhoshkumar and A. Yusuf. In silico structural modeling and analysis of physicochemical properties of curcumin synthase (CURS1, CURS2, and CURS3) proteins of *Curcuma longa*. *Journal of Genetic Engineering and Biotechnology* 18(1): 24 (2020). <https://doi.org/10.1186/s43141-020-00041-x>
- 33. M.H.U. Masum, A.A. Mahdeen, L. Barua, R. Parvin, H.P. Heema, and J. Ferdous. Developing a chimeric multiepitope vaccine against Nipah virus (NiV) through immunoinformatics, molecular docking and dynamic simulation approaches. *Microbial Pathogenesis* 197: 107098 (2024). <https://doi.org/10.1016/j.micpath.2024.107098>
- 34. A. Alibakhshi, A.A. Bahrami, E. Mohammadi, S. Ahangarzadeh, and M. Mobasher. In silico design of a new multi-epitope vaccine candidate against SARS-CoV-2. *Acta Virologica* 67: 12481 (2024). <https://doi.org/10.3389/av.2023.12481>
- 35. N. Rapin, O. Lund, M. Bernaschi, and F. Castiglione. Computational immunology meets bioinformatics: the use of prediction tools for molecular binding in the simulation of the immune system. *PLOS One* 5(4): e9862 (2010). <https://doi.org/10.1371/journal.pone.0009862>
- 36. R. Khandia, S. Singhal, U. Kumar, A. Ansari, R. Tiwari, K. Dhama, J. Das, A. Munjal, and R.K. Singh. Analysis of Nipah virus codon usage and adaptation to hosts. *Frontiers in Microbiology* 10: 886 (2019). <https://doi.org/10.3389/fmicb.2019.00886>
- 37. K. Li, S. Yan, N. Wang, W. He, H. Guan, C. He, Z. Wang, M. Lu, W. He, and R. Ye. Emergence and adaptive evolution of Nipah virus. *Transboundary and Emerging Diseases* 67(1): 121-32 (2020). <https://doi.org/10.1111/tbed.13330>
- 38. A. Kumar, G. Misra, S. Mohandas, and P.D. Yadav. Multi-epitope vaccine design using in silico analysis of glycoprotein and nucleocapsid of Nipah virus. *PLOS One* 19(5): e0300507 (2024). <https://doi.org/10.1371/journal.pone.0300507>
- 39. E.C. Banico, E.M.J.S. Sira, L.E. Fajardo, A.N.G. Dulay, N.M.O. Odchimar, A.M. Simbulan, and F.L. Orosco. Advancing one health vaccination: in silico design and evaluation of a multi-epitope subunit vaccine against Nipah virus for cross-species immunization using immunoinformatics and molecular modeling. *PLOS One* 19(9): e0310703 (2024). <https://doi.org/10.1371/journal.pone.0310703>
- 40. A. Albutti. An integrated multi-pronged reverse vaccinology and biophysical approaches for identification of potential vaccine candidates against Nipah virus. *Saudi Pharmaceutical Journal* 31(12): 101826 (2023). <https://doi.org/10.1016/j.jsps.2023.101826>
- 41. S. Sharma, P.D. Yadav, and S. Cherian. Comprehensive immunoinformatics and bioinformatics strategies for designing a multi-epitope-based vaccine targeting structural proteins of Nipah virus. *Frontiers in Immunology* 16: 1535322 (2025). <https://doi.org/10.3389/fimmu.2025.1535322>